Workshop on Visualisation in Environmental Sciences (EnvirVis) (2017)
R. Bujack and A. Middel and K. Rink and D. Zeckzer (Editors)

Visual Eddy Analysis of the Agulhas Current

F. Raith[1], N. Röber[2], H. Haak[3] and G. Scheuermann[1]

[1] Institute of Computer Science, Leipzig University, Germany
[2] Deutsches Klimarechenzentrum, Hamburg, Germany
[3] Max-Planck-Institut für Meteorologie Hamburg, Germany

Abstract

Large mesoscale eddies in the ocean can transport a substantial amount of heat and salt over large distances. Using high-resolution ICON ocean simulation data, it is possible to detect and track eddies in the ocean and analyze their pathway. In this paper, we focus on the area of the Agulhas Current at the southern tip of Africa and present our results for eddy detection and eddy tracking. The Agulhas Current transports warm and salty water from the Indian Ocean towards the South Atlantic Ocean before it makes a strong turn back into the Indian Ocean. Some eddies associated with this current do not follow this turn back into the Indian Ocean, but travel north-west deeper up the Atlantic. We show how such eddies can be detected and tracked in the ICON model and how far some of them travel over the duration of one year. We also indicate which types of eddies follow these paths and give a visual analysis of eddy properties like volume and temperature.

Categories and Subject Descriptors (according to ACM CCS): •Human-centered computing → Scientific visualization; Geographic visualization; •Computing methodologies → Scientific visualization;

1. Introduction

The Agulhas Current System (ACS) in the south-western Indian Ocean is an important part of the 'warmwater route' of the Global Conveyor Belt Circulation that connects all ocean basins. The ACS transports large amounts of heat, salt and bio-geo-chemical tracers from the southern Indian Ocean into the South Atlantic. Its complex flow field consists of boundary currents and current separations (Agulhas Current), retroflections (Agulhas Return Current) and mesoscale eddies (Agulhas Rings). The latter form the so called Agulhas Leakage and are responsible for the exchange between both basins. Agulhas Rings and Agulhas Leakage are subject to ongoing oceanographic research [Bea11]. Of particular interest is their role in the stability of the ocean Conveyor Belt Circulation. A realistic representation of the ACS and its components is a challenge for numerical ocean modeling.

In our work we use data from a global ICOsahedral Nonhydrostatic (ICON) ocean simulation and identify and track eddies to gain information about their pathways, as well as the volume, heat and salt that is transported. Finally, we visualize the recognized pathways and eddies for easy access by oceanographers.

2. Related Work

In the literature, there is already a number of ocean eddy studies. These are differentiated by the climate simulation data used and the methods for identification of ocean eddies. In the following, we give a short overview of the most relevant contributions.

Woodring et al. [WPS*16] use the Model for Prediction Across Scales (MPAS) ocean model and an in situ method for the detection of eddies in the complete ocean. They compare in situ workflow and post-processing workflow with regard to the storage and I/O time bottlenecks, since the effort is very high for global simulations. The eddy detection is performed with the Okubo-Weiss parameter and results vary greatly with regard to the grid cell size.

Daisuke et al. [DFYH16] use the Ocean general circulation model for the Earth Simulator (OFES). Here, the approach is to compare eddies and the surrounding flow field. Based on their interaction, a classification is created and applied. The eddy detection is performed by a new hybrid method from sea surface height (SSH), the velocity field and the Okubo-Weiss parameter on the ocean surface.

Petersen et al. [PWM*13] create a three-dimensional eddy detection in global ocean simulation data using the Community Earth System Model (CESM). The aim is to examine the depth of the eddies. The Okubo-Weiss parameter and a check with the R^2 method are used for the detection. The result is that the predominant majority of the eddies extend over the entire sea depth.

Williams et al. [WHP*11] tried to improve the eddy detection by means of a new circulation criterion, the four corners method. The climate simulation data is given by the Parallel Ocean Program (POP). With this circulation criterion, it is possible to remove false positive eddies which are detected by the Okubo-Weiss parameter.

In contrast to the approaches in the literature, we perform the

DOI: 10.2312/envirvis.20171100

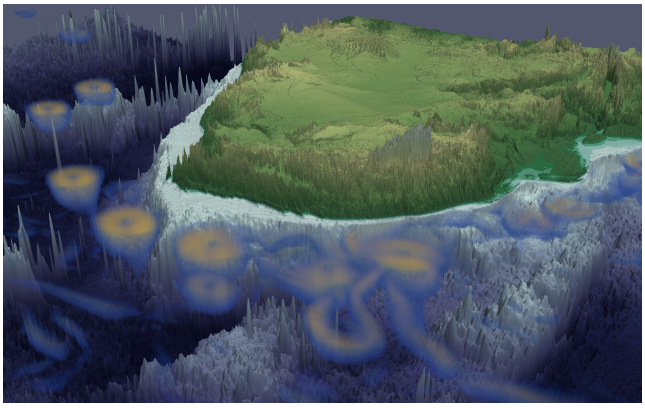

Figure 1: *Data visualization of the velocity magnitude using volume rendering in ParaView.*

eddy detection with data represented in the novel ICON model. Furthermore, the focus is not only on the detection but also on the tracking of the eddies and the visualization of the resulting paths. We visualize the eddies on the sea surface (two-dimensional case) as well as over the entire sea depth (three-dimensional case). Also, we take the direction of rotation of the eddies into account and obtain new knowledge from this.

3. ICON Ocean Model

ICON is jointly developed by the Max Planck Institute for Meteorology (MPI-M) and the German Weather Service (DWD). It is a framework defined on an icosahedron with an equal area projection. ICON and its dynamical core are not only designed to more efficiently utilize current supercomputing systems, but also allow a better coupling between ocean and atmosphere/land components, as well as permit nesting in local regions. The dynamical core of ICON fully solves the compressible non-hydrostatic equations of motion for high spatial resolutions. The model data is sampled on a dual lattice, consisting of triangular and hexagonal cells, allowing C-grid type discretization and a refinement in local areas [ZRRB15]. Although the horizontal layout can be considered irregular, the vertical grid is regular with unequal cell sizes. Cells close to the Earth's surface are usually thinner than those high in the atmosphere or deep in the ocean. Similar models to ICON – in terms of grid layout and structure – are the American MPAS, and the Japanese Non-hydrostatic ICOsahedral Atmospheric Model (NICAM) [RPH*13, PJR*15, SMT*07].

The data used in this research originates from a high resolution (10 km) eddy-resolving global ICON ocean simulation run. The data is written out as daily average for several 3D quantities, such as horizontal velocities, temperature and salinity. To reduce the data in size, we focus on a larger area at the southern tip of Africa that includes the Agulhas Current, see also Figure 1.

4. Eddy Detection and Tracking

We have chosen to use a method based on thresholds of the Okubo-Weiss parameter and the four corners method to identify eddies in the ocean. The first step in eddy detection is to identify the potential eddies in the velocity field with the Okubo-Weiss parameter and its threshold. Next we verify the potential eddies with the four corners method. In the three-dimensional case, we also use eddy size. As a last step, the time-dependent data is used to track eddies through spatial overlap.

In detail, the Okubo-Weiss parameter of Okubo [Oku70] and Weiss [Wei91] is the two-dimensional equivalent of the Q-criterion. The method is applied to identify eddies on the sea surface. The Okubo-Weiss parameter is defined on the velocity field as,

$$\mathrm{OW} = s_n^2 + s_s^2 - \omega^2, \tag{1}$$

where s_n is the normal strain, s_s is the shear strain and ω the vorticity. Expressed in terms of velocity gradients, the following formula result

$$\mathrm{OW} = \left(\frac{\partial u}{\partial x} - \frac{\partial v}{\partial y}\right)^2 + \left(\frac{\partial v}{\partial x} + \frac{\partial u}{\partial y}\right)^2 - \left(\frac{\partial v}{\partial x} - \frac{\partial u}{\partial y}\right)^2, \tag{2}$$

where u is the east-west velocity component, v the north-south velocity component, and x and y define the local coordinate system. Consequently two regions can be found with the Okubo-Weiss parameter. On the one hand, negative regions are recognized in which the vorticity dominates; these are vortex cores. On the other hand, positive regions are recognized in which the pressure dominates; these are the vortex rings. The Okubo-Weiss threshold,

$$\frac{\mathrm{OW}}{\sigma_{\mathrm{OW}}} \leq -0.2, \tag{3}$$

where σ_{OW} is the standard-deviation of the Okubo-Weiss field and -0.2 is the typical threshold value, is used for the detection of the eddy cores. This threshold is also used by Woodring et al. [WPS*16] and Williams et al. [WHP*11]. We do not calculate the standard deviation for each time step, but use a global value for all time steps to take into account the similarities of the eddies.

Since the Okubo-Weiss parameter detects too many false positive eddies, the results must then be verified. The four corners method of Williams et al. [WHP*11] is used mainly for this verification. This verifies whether an eddy rotates completely. For this purpose, we calculate an angle between each velocity vector of the points in the eddies and a vector oriented towards the east. These angles are sorted into one of the four angle ranges northeast (0° – 90°), northwest (90° – 180°), southwest (180° – 270°) and southeast (270° – 360°). In addition, each angle range must be contained in an eddy to a certain percentage. We use 8% as defined by Williams et al. [WHP*11].

The eddies are additionally verified with eddy size in the three-dimensional case. This is used to remove eddies that is too small. As in the paper of Woodring et al. [WPS*16], 100 cells is assumed as the minimum size for eddies.

Time-dependent data is used for tracking. The tracking of an eddy between time steps is done by searching for overlaps. The point clouds of two eddies must overlap in such a way that one of them contains over 50% of the other. In order to prevent incorrect assignments, the direction of rotation must also be the same. The matched eddies are removed from the dataset to prevent duplicate assignments.

In order to improve the recognition of unstable eddies and identify the forming and dissolving regions, the eddies are tracked forward and backward in time. Additional each eddy has to sucessfully pass the verification of the eddy detection in one time step only once.

The eddy detection and tracking can be performed selectively for the two-dimensional case as well as for the three-dimensional case. This is possible since the calculation of the Okubo-Weiss parameter requires only the surface velocity vectors. In this work, the two-dimensional case is calculated for a depth of 67 m. This is the first available layer below 60 m and, according to Skyllinggstad et al. [SS00], an active mixing takes place by the wind up to 60 m depth. This mixing means that the observed water velocities are influenced by the atmospheric wind which would interfere with our eddy detection.

5. Results and Discussion

The data analysis took place at a local workstation with an Intel Core i7 – 980 CPU, 6 cores, running at 3.33 GHz, 24 GB RAM and an NVIDIA GeForce GTX 580 GPU. The analysis was implemented using the FAnToM framework [WGH*09, fan16].

For visual analysis, the eddies are classified according to their rotation to detect possible differences. The eddies are grouped by their mathematically rotation direction into two different sets, i.e., positive and negative.

When displaying the eddy pathways, we observed that only the positive eddies are stable over a longer period of time. This leads to the assumption that these are mainly responsible for transport. This higher stability can be detected in two-dimensional and three-dimensional cases. In Figure 2, the eddy pathways of the most stable eddies are displayed for the two-dimensional case. The color of the eddies represents age. A step length of 20 days is assumed, as, according to the work of Kang et al. [KC13], this is the time an eddy needs to achieve its maximum size. It is evident that the most stable eddies are formed in the Agulhas Current and move from the Indian Ocean to the Atlantic Ocean.

This can also be used to draw a conclusion on the distance traveled and the velocity. In Tables 1 and 2, it can be discerned that positive eddies have a higher median travel distance, but, at the same time, their median velocity is lower than negative eddies. This indicates that the positive eddies are more stable, but move slower. From the tables and also the examination of the eddy pathways, it can be seen that the tracking of the eddies in the three-dimensional case still requires improvements.

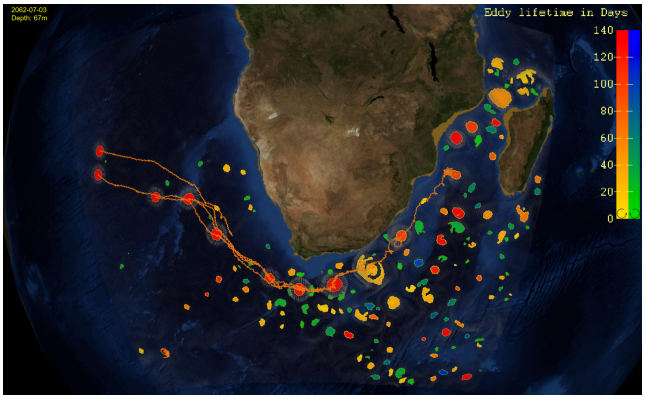

Figure 2: *Display of the detected eddy pathways for 2062-07-03 in two-dimensional case*

Table 1: *Distance of the eddies for all cases divided by direction of rotation*

	Direction of rot.	2D Case	3D Case
Minimum	**Positive**	0 km	0 km
Median		242.56 km	167.67 km
Maximum		6147.98 km	5611.1 km
Minimum	**Negative**	0 km	0 km
Median		184.15 km	146.37 km
Maximum		7087.49 km	10434.87 km

Table 2: *Velocity of the eddies for all cases divided by direction of rotation*

	Direction of rot.	2D Case	2D Case
Minimum	**Positive**	0 km/d	0 km/d
Median		9.63 km/d	10.12 km/d
Maximum		74.75 km/d	136.4 km/d
Minimum	**Negative**	0 km/d	0 km/d
Median		10.92 km/d	13.23 km/d
Maximum		73.22 km/d	88.46 km/d

Next, we examined the volume of the eddies in the three-dimensional case. In Figure 3, the eddies are displayed as cylinders whose radius reflects the volume. This representation facilitates the perception of the relevant eddies. The visualization demonstrates that the positive eddies have a greater volume.

With the additional investigation of the depth in Figure 4, it could also be established that the positive eddies are shallower than the negative eddies. With a closer look, we found that our filtering by

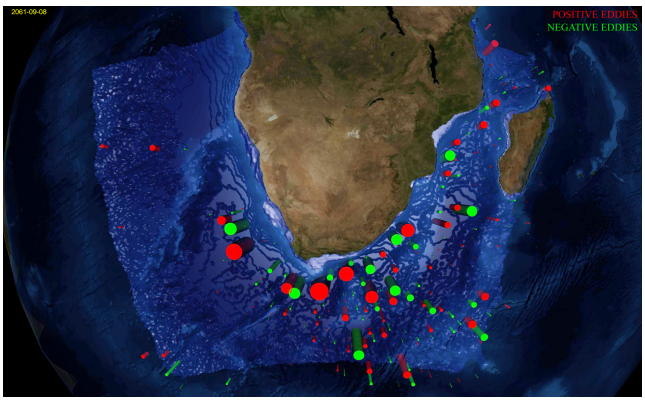

Figure 3: *Display of the volume of the eddies in the radius cylinder representation from above in the three-dimensional case for 2061-09-08*

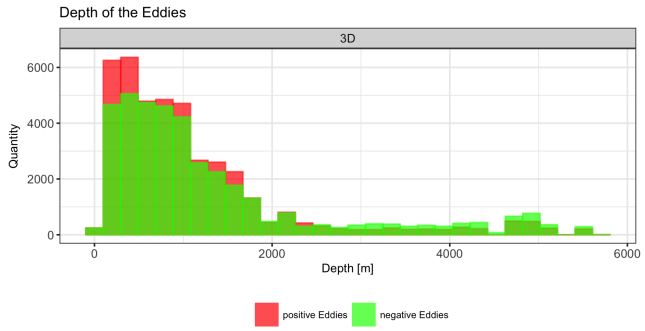

Figure 4: *Depth of the detected eddies over all time steps in the three-dimensional case*

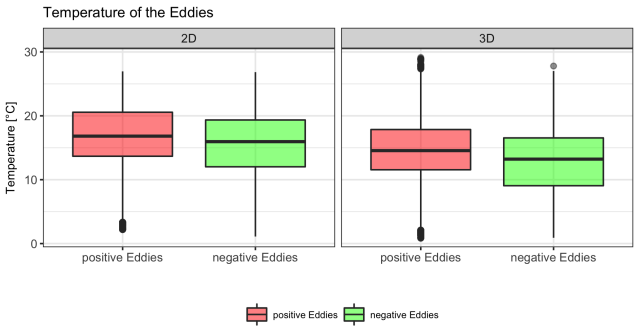

Figure 6: *Temperature of the detected eddies over all time steps in two-dimensional case (left) and in the three-dimensional case (right)*

eddy size removes eddies with larger depths. This indicates that we still have trouble finding eddies in large ocean depths.

In Figure 5, the largest eddies are colored according to their temperature while cylinder radius shows volume. In comparison with Figure 3, it is well recognizable that the positive eddies have a higher temperature and travel from the Indian into the Atlantic Ocean. This is also reflected in Figure 6, where the temperature is compared over all time steps. This behaviour is found in both two-dimensional and the three-dimensional case analyses.

By considering the individual results, it can be concluded that the two-dimensional case is a very good illustration of the three-dimensional case. This is also confirmed by comparison with the results of Petersen et al. [PWM*13]. We faced problems with our approach only while tracking eddies in the three-dimensional cases. Another problem is the detection of eddies in the deep sea. For this region, there are hardly any eddies found, which is in contrast to results of Petersen et al. [PWM*13], who described eddies in deep sea as a frequent phenomenon. Further investigation is required to resolve this issue.

The most important result of our investigation is that only eddies

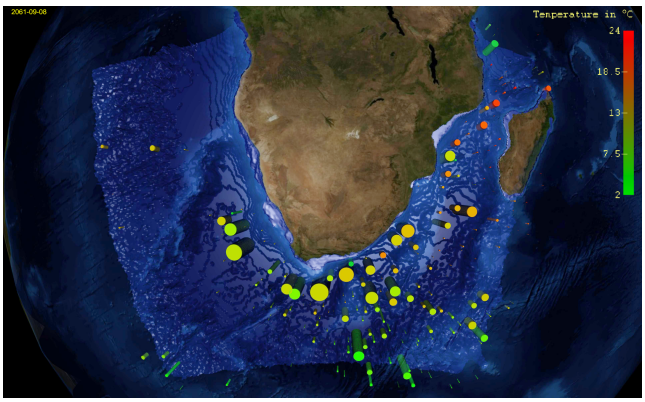

Figure 5: *Radius cylinder representation of the temperature from all eddies in the three-dimensional case for 2061-09-08*

with a positive rotation direction transport mass and energy over large distances in the observed region.

6. Conclusions and Future Work

This paper presented an extended model for eddy detection which includes the tracking of eddies over time. We used this method to study the Agulhas Current because a large number of eddies are created in the region and some travel far away from the current. The aim was to gain a simplified access to the data by means of a visual analysis. New insights were gained about the direction of rotation and the possible transport in the region.

In future work, several areas can be expanded, e.g. better visual presentation, better detection and tracking, and comparison to other regions. For example, one could improve the eddy detection by using the R^2 method from Petersen et al. [PWM*13] or consider SSH to verify detected eddies as in the work of Daisuke et al. [DFYH16] or Yi et al. [YDHZ14]. Eddy tracking can be improved by using mean eddy velocity for prediction. Currently, we are not able to display all data generated during calculation in one visualization. Therefore, the selection of individual eddies would be a conceivable application to display more targeted information.

The next step is to apply the workflow on a much bigger target area than presented in this work. This could further improve the added value of the model for climate research, as it could be used to explore the impact of eddies on a global scale. In particular, an implementation of the workflow which is usable on the high-performance computers of the DKRZ is envisioned.

Acknowledgement

This work was funded by the German Federal Ministry of Education and Research within the project Competence Center for Scalable Data Services and Solutions (ScaDS) Dresden/Leipzig (BMBF 01IS14014B).

References

[Bea11] BEAL, L.M., DE RUIJTER, W.P.M., BIASTOCH, A., ZAHN, R.: On the role of the Agulhas system in ocean circulation and climate. *Nature* (2011). 1

[DFYH16] DAISUKE M., FUMIAKI A., YUMI I., HIDEHARU S.: A New Approach to Ocean Eddy Detection Tracking and Event Visualization. *Procedia Computer Science 80* (January 2016). 1, 4

[fan16] About FAnToM | FAnToM - Field Analysis using Topological Methods. https://www.informatik.uni-leipzig.de/fantom/content/about-fantom, October 2016. 3

[KC13] KANG D., CURCHITSER E. N.: Gulf Stream eddy characteristics in a high-resolution ocean model. *Journal of Geophysical Research: Oceans 118* (April 2013). 3

[Oku70] OKUBO A.: Horizontal dispersion of floatable particles in vicinity of velocity singularities such as convergences. *Deep-Sea Research I 17* (1970). 2

[PJR*15] PETERSEN M. R., JACOBSEN D. W., RINGLER T. D., HECHT M. W., MALTRUD M. E.: Evaluation of the arbitrary Lagrangian-Eulerian vertical coordinate method in the MPAS-Ocean model. *Ocean Modelling 86* (2015), 93–113. 2

[PWM*13] PETERSEN M. R., WILLIAMS S. J., MALTRUD M. E., HECHT M. W., HAMANN B.: A three-dimensional eddy census of a high-resolution global ocean simulation. *Journal of Geophysical Research: Oceans 118* (April 2013). 1, 4

[RPH*13] RINGLER T., PETERSEN M., HIGDON R., JACOBSEN D., JONES P., MALTRUD M.: A multi-resolution approach to global ocean modeling. *Ocean Modelling 69* (2013), 211–232. 2

[SMT*07] SATOH M., MATSUNO T., TOMITA H., MIURA H., NASUNO T., IGA S.: Nonhydrostatic Icosahedral Atmospheric Model (NICAM) for global cloud resolving simulations. *Computational Physics, special issue on Predicting Weather, Climate and Extreme events 227* (2007), 3486–3514. 2

[SS00] SKYLLINGSTAD E. D., SMYTH W. D.: Resonant Wind-Driven Mixing in the Ocean Boundary Layer. *Journal of Physical Oceanography 30* (August 2000). 3

[Wei91] WEISS J.: The dynamics of enstrophy transfer in two-dimensional hydrodynamics. *Physica D 48* (1991). 2

[WGH*09] WIEBEL A., GARTH C., HLAWITSCHKA M., WISCHGOLL T., SCHEUERMANN G.: Fantom-lessons learned from design, implementation, administration, and use of a visualization system for over 10 years. 3

[WHP*11] WILLIAMS S., HECHT M., PETERSEN M., STRELITZ R., MALTRUD M., AHRENS J., HLAWITSCHKA M., HAMANN B.: Visualization and Analysis of Eddies in a Global Ocean Simulation. *Computer Graphics Forum 30*, 3 (2011). 1, 2

[WPS*16] WOODRING J., PETERSEN M., SCHMEIÃ§ER A., PATCHETT J., AHRENS J., HAGEN H.: In Situ Eddy Analysis in a High-Resolution Ocean Climate Model. *IEEE Transactions on Visualization and Computer Graphics 22*, 1 (January 2016). 1, 2

[YDHZ14] YI J., DU Y., HE Z., ZHOU C.: Enhancing the accuracy of automatic eddy detection and the capability of recognizing the multi-core structures from maps of sea level anomaly. *Ocean Science 10* (February 2014). 4

[ZRRB15] ZÄNGL G., REINERT D., RÍPODAS P., BALDAUF M.: The ICON (ICOsahedral Non-hydrostatic) modelling framework of DWD and MPI-M: Description of the non-hydrostatic dynamical core. *Quarterly Journal of the Royal Meteorological Society 141*, 687 (2015), 563–579. 2